BIOCHEMISTRY
including biophysical chemistry & molecular biology

Article

pubs.acs.org/biochemistry

Decoy Plasminogen Receptor Containing a Selective Kunitz-Inhibitory Domain

Yogesh Kumar,[†,#] Kanagasabai Vadivel,[†,#] Amy E. Schmidt,[‡,#] Godwin I. Ogueli,[†] Sathya M. Ponnuraj,[†] Nalaka Rannulu,[§] Joseph A. Loo,[§,∥] Madhu S. Bajaj,[⊥] and S. Paul Bajaj*[,†,∥]

[†]Department of Orthopaedic Surgery, UCLA School of Medicine, Los Angeles, California 90095, United States

[‡]Department of Pathology and Laboratory Medicine, Indiana University School of Medicine, Indianapolis, Indiana 46202, United States

[§]Department of Chemistry and Biochemistry, UCLA, Los Angeles, California 90095, United States

[∥]Molecular Biology Institute, UCLA, Los Angeles, California 90095, United States

[⊥]Department of Medicine, Division of Pulmonary, and Critical Care Medicine, David Geffen School of Medicine, UCLA, Los Angeles, California 90095, United States

Supporting Information

ABSTRACT: Kunitz domain 1 (KD1) of tissue factor pathway inhibitor-2 in which P2′ residue Leu17 (bovine pancreatic trypsin inhibitor numbering) is mutated to Arg selectively inhibits the active site of plasmin with ∼5-fold improved affinity. Thrombin cleavage (24 h extended incubation at a 1:50 enzyme-to-substrate ratio) of the KD1 mutant (Leu17Arg) yielded a smaller molecule containing the intact Kunitz domain with no detectable change in the active-site inhibitory function. The N-terminal sequencing and MALDI-TOF/ESI data revealed that the starting molecule has a C-terminal valine ($KD1_{L17R}$-V_T), whereas the smaller molecule has a C-terminal lysine ($KD1_{L17R}$-K_T). Because $KD1_{L17R}$-K_T has C-terminal lysine, we examined whether it could serve as a decoy receptor for plasminogen/plasmin. Such a molecule might inhibit plasminogen activation as well as the active site of generated plasmin. In surface plasmon resonance experiments, tissue plasminogen activator (tPA) and Glu-plasminogen bound to $KD1_{L17R}$-K_T ($K_d \sim 0.2$ to 0.3 μM) but not to $KD1_{L17R}$-V_T. Furthermore, $KD1_{L17R}$-K_T inhibited tPA-induced plasma clot fibrinolysis more efficiently than $KD1_{L17R}$-V_T. Additionally, compared to ε-aminocaproic acid $KD1_{L17R}$-K_T was more effective in reducing blood loss in a mouse liver-laceration injury model, where the fibrinolytic system is activated. In further experiments, the micro(μ)-plasmin−$KD1_{L17R}$-K_T complex inhibited urokinase-induced plasminogen activation on phorbol-12-myristate-13-acetate-stimulated U937 monocyte-like cells, whereas the μ-plasmin−$KD1_{L17R}$-V_T complex failed to inhibit this process. In conclusion, $KD1_{L17R}$-K_T inhibits the active site of plasmin as well as acts as a decoy receptor for the kringle domain(s) of plasminogen/plasmin; hence, it limits both plasmin generation and activity. With its dual function, $KD1_{L17R}$-K_T could serve as a preferred agent for controlling plasminogen activation in pathological processes.

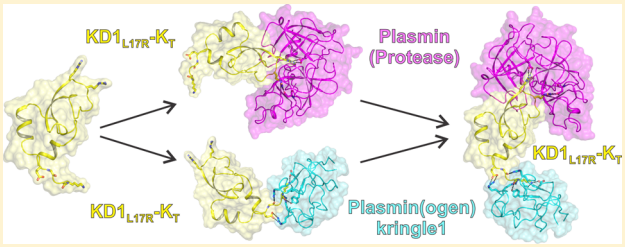

Plasmin is a multifunctional proteolytic enzyme (MW 92 000) that circulates in blood as a single-chain inactive zymogen, plasminogen.[1] Although plasminogen is expressed ubiquitously in the body,[2] hepatocytes represent the predominant site of its synthesis.[3,4] Circulating plasminogen has an N-terminal glutamic acid (Glu−Plg) and contains a PAN/apple domain, five kringle domains, and the C-terminal latent serine protease domain.[5] Native plasminogen exists in a tight conformation in which the PAN/apple domain is bound to the kringle 5 domain.[6,7] Upon cleavage of the Arg561−Val562 scissile bond, single-chain plasminogen is converted to a disulfide-linked two-chain active protease, plasmin.[8,9] The heavy chain of Glu-plasmin consists of the PAN/apple domain and five kringle domains, whereas the light chain contains the C-terminal protease domain.[9] Plasminogen can be activated by either urokinase plasminogen activator (uPA) or tissue plasminogen activator (tPA).[9−11] Through self-catalysis, Lys-plasmin (and Lys-plasminogen) is formed that lacks the PAN/apple domain.[5,8] Because of the absence of interaction(s) between the PAN/apple domain and the kringle 5 domain, Lys-plasminogen exist in a more open conformation than Glu−Plg.[12,13] Importantly, Lys-plasminogen is more readily activated by plasminogen activators as compared to Glu−Plg.[14,15] Plasminogen activators, tPA and uPA, are inhibited by plasminogen activator inhibitor-1 (PAI-1)[16] and PAI-2,[17,18] whereas plasmin is inhibited by α_2-antiplasmin[19] and α_2-macroglobulin.[20]

Received: September 17, 2013
Revised: December 31, 2013
Published: January 2, 2014

Plasmin plays an important role in fibrinolysis and is responsible for clot lysis at the site of thrombus formation.[9] During fibrinolysis, plasminogen is primarily activated by tPA, which is released from the damaged endothelium.[21,22] Starting at the N-terminus, tPA consists of a finger domain, an epidermal growth factor-like domain, two kringle domains, and a C-terminal protease domain.[23,24] The finger domain and the second kringle domain of tPA bind to the C-terminal lysine residues exposed in the thrombus clot.[25,26] Plasminogen is also localized to the fibrin clot via its kringle domains 1 and 4, where tPA locally converts it to plasmin.[27] During degradation of fibrin, plasmin generates additional C-terminal lysine residues, which enhances tPA and plasminogen/plasmin binding to the clot for efficient lysis.[28] Furthermore, as compared to the circulating plasmin, fibrin-bound plasmin is poorly inhibited by α_2-antiplasmin.[21] Thus, such a localized mechanism of fibrinolysis prevents degradation of circulating fibrinogen.

In severe trauma[29] and during major surgical procedures, such as cardiac surgery, the fibrinolytic system is hyperactivated.[30,31] In trauma, uncontrolled bleeding is the leading cause of preventable death.[32] Antifibrinolytic agents when used prophylactically can significantly reduce blood loss and the need for extensive blood transfusions.[30,33,34] Aprotinin (bovine pancreatic trypsin inhibitor, BPTI), a potent inhibitor of the plasmin active site, has been the leading antifibrinolytic agent used to prevent blood loss in cardiovascular bypass surgery.[35] However, because of its side effects such as kidney damage, myocardial infarction, and anaphylactic potential, it has been removed from the clinical market.[36−38] The presently used antifibrinolytic agents are tranexamic acid (TE) and ε-aminocaproic acid (εACA);[39] both of these lysine analogues are less effective than aprotinin and are also associated with kidney failure and seizures.[39,40] Thus, a molecule with superior efficacy is desirable for use an antifibrinolytic agent.

The plasminogen system also plays an essential role in pericellular proteolysis-dependent degradation of the extracellular matrix (ECM)[41−46] and activation of cytokines.[47] Plasmin activates several pro-matrix metalloproteases (proMMPs), including proMMPs 3, 9, 12, and 13,[48,49] that degrade other matrix components such as collagens.[50,51] Furthermore, plasmin plays a significant role in angiogenesis by releasing certain matrix-associated growth factors such as fibroblast growth factor and vascular endothelial growth factor[52,53] as well as in the activation of latent transforming growth factor-β.[54] Thus, plasmin is involved in inflammation, wound healing, cell migration, tumor growth, and apoptosis.[9] All of these functions are attributed to uPA (in association with uPA receptor)-mediated activation of plasminogen bound to the cell surface receptors present on monocytes/macrophages, smooth muscle cells, endothelial and epithelial cells, keratinocytes, and fibroblasts as well as platelets.[55] Plasminogen receptors with C-terminal lysine residues are abundantly expressed by different cell types,[56−58] and invasive properties of tumor cells are dependent on plasmin-mediated proteolysis of ECM.[59,60] Thus, attenuating plasminogen activation by preventing its binding to the cell surface receptors and inhibiting the formed plasmin could be an attractive target for controlling these pathological processes.

Tissue factor pathway inhibitor-2 (TFPI-2), also known as placental protein 5 or matrix serine protease inhibitor, contains three Kunitz-type inhibitory domains in tandem.[61−63] Kunitz domain 1 (KD1) of TFPI-2 is the only inhibitory domain, and it inhibits plasmin, factor (F) XIa, plasma kallikrein (pKLK), and FVIIa/tissue factor.[64] Using serine protease subsite S2′/P2′ profiling,[65] we designed a variant KD1-L17R molecule that is a much more potent inhibitor of plasmin; furthermore, it does not inhibit pKLK or FXIa.[66] (For KD1 and BPTI residue numbering, KD1 and BPTI residues P2, P1, P1′, and P2′ are numbered according to Schechter and Berger.[65] The corresponding subsites are S2, S1, S1′, and S2′ in the enzyme, respectively. The residue numbering corresponds to BPTI such that residue 15 is at the P1 position and residue 17 is at the P2′ position. For comparison, KD1 is numbered using the BPTI numbering system such that residues 15 and 17 in BPTI correspond to residues 24 and 26 in KD1, respectively. Thus, the residues in KD1 differ by nine from BPTI.) The *Escherichia coli* expressed KD1-L17R[66] has a C-terminal valine and nine residues at the N-terminus that are not part of the Kunitz domain; it is termed here as $KD1_{L17R}$-V_T. (For the $KD1_{L17R}$-V_T designation, $KD1_{L17R}$-V_T contains residues 1−73 of human TFPI-2; it also has four additional residues (Gly-Ser-His-Met) at the N-terminus that were introduced during cloning. It has a C-terminal valine residue.[66]) In this article, we obtained a smaller molecular species that has C-terminal lysine and lacks the first 7−9 residues; it is referred to as $KD1_{L17R}$-K_T. (For the $KD1_{L17R}$-K_T designation, approximately 80% of the $KD1_{L17R}$-K_T contains residues 8−72, and the remaining 20% has residues 10 (residue 1 in BPTI)−72 of human TFPI-2; it has a C-terminal lysine residue. Here, these two species are collectively referred to as $KD1_{L17R}$-K_T.) Structural and functional characterization of $KD1_{L17R}$-K_T, including its inhibition of plasmin and binding to the kringle domains of plasminogen, are presented here. $KD1_{L17R}$-K_T with its dual function might be a preferred agent for controlling plasmin generation and its inhibition in pathological processes.

EXPERIMENTAL PROCEDURES

Materials. *E. coli* strain BL21(DE3) pLysS and the pET28a expression vector were obtained from Novagen Inc. (Madison, WI). Amicon centrifugal filter devices (3000 M_r cutoff) were purchased from Millipore (Bedford, MA). Q-Sepharose FF, SP-Sepharose FF, Superdex-200, and His-Trap HP columns were obtained from Amersham Biosciences. Kanamycin, isopropyl thiogalactopyranoside (IPTG), and 12-*O*-tetradecanoylphorbol-13-acetate (PMA) were obtained from Sigma. Human α-thrombin (IIa), FXIa, *p*KLK, and plasmin were purchased from Haematologic Technologies Inc. tPA (Alteplase) was purchased from Genentech (South San Francisco, CA). uPA was obtained from Calbiochem, EMD Biosciences Inc. (San Diego, CA). Glu−Plg was obtained from Enzyme Research Laboratories (South Bend, IN). εACA (Amicar) was obtained from ICN Biomedicals Inc. (Aurora, OH). Normal pooled plasma (NPP) was purchased from George King Bio-Medical Inc. (Overland Park, KS). Plasmin substrate S-2251 (H-D-Val-Leu-Lys-*p*-nitroanilide) and *p*KLK and FXIa substrate S-2366 (pyroGlu-Pro-Arg-*p*-nitroanilide) were obtained from Diapharma Inc. All other reagents were of the highest purity commercially available.

Expression and Purification of $KD1_{L17R}$-V_T. Residues 1−73 of human TFPI-2 containing the KD1 cDNA sequence were cloned and overexpressed as an N-terminal His_6-tagged fusion protein in *E. coli* strain BL21(DE3) pLysS using the T7 promoter system.[66−69] Point mutant $KD1_{L17R}$-V_T was generated using the QuikChange site-directed mutagenesis kit (Stratagene, La Jolla, CA). His_6-tagged $KD1_{L17R}$-V_T was expressed in *E. coli* grown in Luria broth containing 15 mg/L

of kanamycin and induced at 37 °C with 1 mM IPTG. His_6-tagged $KD1_{L17R}$-V_T was purified from the inclusion bodies and refolded as described.[66,68−70]

Purified His_6-tagged $KD1_{L17R}$-V_T was digested with IIa at a 1:1000 enzyme/substrate molar ratio for 2 h at 37 °C. Complete digestion of KD1 by IIa was confirmed by SDS-PAGE analysis of temporal aliquots.[69] His_6-tag-free protein was separated from the His_6 tag and IIa using Superdex-200 gel-filtration chromatography equilibrated with 50 mM Tris-HCl, pH 7.5, containing 100 mM NaCl (TBS).[66] The preparation was characterized with respect to protein concentration using an extinction coefficient (A_{280}) of 2.45 at 1 mg/mL, purity (SDS-PAGE), N-terminal sequence, and mass spectrometry prior to its use in biochemical experiments.

Preparation and Isolation of $KD1_{L17R}$-K_T. Incubation of $KD1_{L17R}$-V_T (1 mg/mL in TBS at pH 7.5) with IIa at a 1:50 enzyme/substrate molar ratio for 24 h at 37 °C resulted in a smaller $KD1_{L17R}$-K_T molecular species. $KD1_{L17R}$-K_T was separated from IIa using Superdex-200 gel-filtration chromatography equilibrated with TBS, pH 7.5.[66] Purified $KD1_{L17R}$-K_T was characterized with respect to protein concentration using an extinction coefficient (A_{280}) of 2.84 at 1 mg/mL, purity (SDS-PAGE), N-terminal sequence, and mass spectrometry prior to its use in biochemical experiments.

SDS-PAGE. SDS-PAGE was performed using the Laemmli buffer system.[71] The acrylamide concentration used was between 10 and 15%, and the gels were stained with Coomassie Brilliant Blue dye.

Amino Acid Sequence Analysis and Mass Spectrometry. For N-terminal sequence analysis, proteins were transferred to the polyvinylidene difluoride membrane from the reduced SDS-PAGE gel. Automated N-terminal protein sequencing was performed using a pulsed-liquid solid-phase sequenator with online phenylthiohydantoin (PTH)-amino acid analysis (Applied Biosystems cLC system) at the UCLA Biopolymer Core facility. Mass spectrometry (MS) data were collected by matrix-assisted laser desorption ionization (MALDI)-MS and electrospray ionization (ESI)-MS. The protein solution was desalted and concentrated prior to MS measurements using reversed-phase media packed into pipet tips (C4-resin ZipTip, Millipore, Billerica, MA). A Voyager DE-STR MALDI time-of-flight mass spectrometer (Applied Biosystems, Foster City, CA) operating in the linear mode was used for the MALDI-MS measurements. The protein sample solution (0.5 μL) was spotted onto a stainless steel sample plate followed by 0.5 μL of the MALDI matrix solution, α-cyano-4-hydroxycinnamic acid (CHCA). The spotted samples were allowed to dry at room temperature prior to data acquisition. ESI-MS data was collected using a nanospray source and a solariX hybrid 15-T Fourier transform ion cyclotron resonance (FT-ICR) mass spectrometer (Bruker Daltonics, Billerica, MA).

$KD1_{L17R}$-K_T Binding to tPA and Glu−Plg Using Surface Plasmon Resonance (SPR). Binding studies were performed on a Biacore T100 flow biosensor (Biacore, Uppsala, Sweden) at 25 °C. Glu−Plg (~98% purity using SDS-PAGE) or tPA (>98% purity using SDS-PAGE) was immobilized on a carboxymethyl-dextran flow cell (CM5 sensor chips, GE Healthcare) using amine-coupling chemistry. Flow-cell surfaces were activated with a mixture of 1-ethyl-3-(3-dimethylaminopropyl)carbodiimide and *N*-hydroxysulfosuccinimide for 5 min (flow rate of 10 μL/min), after which the protein (20 μg/mL in 10 mM sodium acetate, pH 5.5) was injected onto the surface. Unreacted sites were blocked for 5 min with 1 M ethanolamine. Each analyte ($KD1_{L17R}$-V_T and $KD1_{L17R}$-K_T, 100−2000 nM) was perfused through flow cells in HBS-P buffer (20 mM HEPES, pH 7.4, 100 mM NaCl, and 0.005% (v/v) P20) at 10 μL/min for 6 min. After changing to HBS-P buffer without the protein, analyte dissociation was monitored for 10 min. Flow cells were regenerated with HBS-P containing 20 mM εACA. Data were corrected for nonspecific binding by subtracting signals obtained with the analyte infused through a flow cell without the coupled protein. Binding was analyzed with BIAevaluation software (Biacore) using a 1:1 binding model. K_d values were calculated from the quotient of the derived dissociation (k_d) and association (k_a) rate constants.

Protease Inhibition Assay. All reactions were carried out in TBS, pH 7.5, containing 0.1 mg/mL BSA (TBS/BSA) and 2 mM Ca^{2+} (TBS/BSA/Ca^{2+}, pH 7.5) as described.[66,68] Each enzyme (plasmin, *p*KLK, and FXIa) was incubated with various concentrations (10^{-1} to 2×10^3 nM) of $KD1_{L17R}$-K_T for 1 h at rt in a 96-well microtitration plate (total volume of 100 μL). A synthetic substrate (5 μL) appropriate for each enzyme was then added to a final concentration of 1 K_m, and residual amidolytic activity was measured in a Molecular Devices V_{max} kinetic microplate reader. The inhibition constant, K_i*, was determined using the nonlinear regression data analysis program GraFit. Data for $KD1_{L17R}$-K_T was analyzed with an equation for a tight-binding inhibitor (eq 1) where v_i and v_0 are the inhibited and uninhibited rates, respectively, and $[I]_0$ and $[E]_0$ are the total concentrations of inhibitor and enzyme, respectively.[72,73]

$$v_i = v_0 \frac{((K_i^* + [I]_0 + [E]_0)^2 - 4[I]_0[E]_0)^{1/2} - (K_i^* + [I]_0 - [E]_0)}{2[E]_0} \quad (1)$$

K_i values were obtained by correcting for the effect of substrate according to Beith[72] using eq 2, where $[S]$ is the substrate concentration and K_m is specific for each enzyme.

$$K_i = \frac{K_i^*}{(1 + [S]/K_m)} \quad (2)$$

Fibrinolysis (Clot Lysis) Assay. The method of Sperzel and Huetter[74] was followed with minor modifications as outlined earlier.[66] Briefly, IIa was used to initiate fibrin formation in NPP, and the lysis of the formed clot (fibrinolysis) was induced by simultaneous addition of tPA. Clot formation and lysis were monitored with a Molecular Devices microplate reader (SPECTRAmax 190) measuring the optical density at 405 nm. Briefly, 10 μL of each test compound ($KD1_{L17R}$-V_T, $KD1_{L17R}$-K_T, and εACA) or saline control was added to 240 μL of NPP. Two-hundred twenty-five microliters of this mixture was then added to 25 μL of IIa and tPA in TBS/BSA containing 25 mM $CaCl_2$. In the 250 μL final volume, the concentration of IIa was 0.15 μg/mL and that of tPA was 1 μg/mL. Under control conditions (zero tPA and zero test compound), OD_{405} increased immediately, indicating clotting, followed by an extremely slow decrease, representing fibrinolysis. Because clotting was almost complete after 5 min, fibrinolysis induced by tPA was evaluated as a relative decrease of OD_{405} up to 60 min. $KD1_{L17R}$-V_T (±εACA) and $KD1_{L17R}$-K_T were tested at final concentrations from 2 to 5 μM and εACA (without $KD1_{L17R}$-V_T), from 0.1 to 5 mM.

Mouse Liver-Laceration Model. A protocol using this mouse model to study the efficacy of $KD1_{L17R}$-V_T and of

$KD1_{L17R}$-K_T was approved by the UCLA Chancellor's Animal Research Committee. C57/BL6 mice (8−10 weeks old) weighing ∼20 g were used. Animals were fed standard rodent chow and water and were housed in a vivarium room with normal room temperature and 12 h light−dark cycles. The dosage of $KD1_{L17R}$-V_T or $KD1_{L17R}$-K_T was based on the aprotinin dose used in humans (i.e., 4 μg/g) adjusted for mouse weight.[75] A calculated blood level achieved by this dose was ∼8 μg/mL (∼1 μM). Animals injected with εACA (100 μg/g, calculated blood level of 200 μg/mL or ∼1.3 mM) were used as positive controls, and those receiving saline were used as negative controls. The dosage of εACA was based on the dose used in human protocols.[39,75] Polymixin B-immobilized resin (Detoxi-Gel endotoxin removing gel, Pierce, Rockford, IL) was used to remove lipopolysaccharide from saline, $KD1_{L17R}$-V_T, and $KD1_{L17R}$-K_T. εACA was dissolved at 20 mg/mL in lipopolysaccharide-free saline. Both antifibrinolytic agents and saline were free of lipopolysaccharide, as tested using the Limulus Amebocyte lysates kit (Biowhittaker Inc., Walkersville, MD).

Animals were injected intravenously via the tail vein with the drug in a volume of 100 μL of sterile balanced salt solution immediately preceding anesthesia. Anesthesia was induced and maintained with Isoflurane. The animals were placed on a heating pad in supine position throughout the procedure to maintain the rectal temperature at 37 °C. The abdomen was shaved and prepped. The liver was exposed via an anterior right subcostal incision. The left lobe of the liver was exteriorized by gentle continuous pressure on the left flank posteriorly. A 5 mm transverse incision was made on the left lobe at 1 cm from its inferior edge using a sharp sterile no. 10 scalpel blade. All blood oozing from the site of the left-lobe incision was collected in a sterile, preweighed 3 × 3 cm^2 plastic tray for a total duration of 30 min. Animals were euthanized at the end of the 30 min period.

A factorial one-way analysis of variance (ANOVA) method was used to compare the mean total blood loss in milligrams from the mouse liver across the four treatment groups (saline, εACA, $KD1_{L17R}$-V_T, and $KD1_{L17R}$-K_T). The p value for comparing any two means was computed using a posthoc test under this ANOVA model. Examination of the mean total blood loss error distribution pooled across all four treatments showed that it was normal (Gaussian) after controlling for the effect of treatment. The Shapiro−Wilk goodness of fit test was used to compare formally this distribution to a Gaussian. Thus, no transformations of total blood loss were needed.

Reduction in Glu−Plg Binding to U937 Cell Surface Receptors by Micro(μ)-Plasmin−$KD1_{L17R}$-K_T. Recombinant N-terminal His_6-tagged μ-plasminogen, containing residues 542−791 of the human plasminogen protease domain,[76] was expressed as inclusion bodies using the pET28a vector in *E. coli* strain BL21(DE3). The His_6-tagged μ-plasminogen was isolated using nickel-charged His-Trap column, refolded, and purified using SP-Sepharose FF column as outlined.[76] Isolated μ-plasminogen (1 mg/mL) was digested with IIa to remove the His_6 tag[66] and was activated to μ-plasmin by uPA at a 1:1000 enzyme/substrate molar ratio for 2 h at 37 °C. Removal of the His_6 tag and activation to μ-plasmin was confirmed by reduced SDS-PAGE (15% acrylamide). IIa, uPA, and the His_6 tag were separated from μ-plasmin using a Superdex-200 gel-filtration column.[76] $KD1_{L17R}$-V_T and $KD1_{L17R}$-K_T each was incubated with purified μ-plasmin at a molar ratio of 1.2:1 for 2 h at room temperature. Each complex was then separated from the free $KD1_{L17R}$-V_T or $KD1_{L17R}$-K_T using a Superdex-200 gel-filtration column.[76] Details of the procedure for obtaining the μ-plasmin−$KD1_{L17R}$-V_T or μ-plasmin−$KD1_{L17R}$-K_T complex are described elsewhere (with the crystallization and structure determination of these complexes).

U937 monocyte-like cells were maintained at 37 °C with 5% CO_2 using RPMI-1640 medium supplemented with 10% fetal calf serum as outlined earlier.[77,78] The cells were stimulated with 40 nM PMA for 18 h under sterile conditions as described.[78] The nonadherent cells were recovered by gentle decanting, washed, and suspended in 50 mM Hepes containing 100 mM NaCl and 0.1 mg/mL BSA, pH 7.5 (HBS/BSA, pH 7.5). The cells (10^6/mL, 200 μL) were then incubated at 37 °C for 1 h with 2 μM Glu−Plg containing varying concentrations of μ-plasmin−$KD1_{L17R}$-K_T or μ-plasmin−$KD1_{L17R}$-V_T. The cells were washed and resuspended in 200 μL of HBS/BSA, pH 7.5, and the cell-bound Glu−Plg was activated with 10 nM uPA for 20 min at 37 °C. Each reaction mixture was diluted 10-fold, and the plasmin activity (reflective of bound Glu−Plg) was measured by S-2251 synthetic-substrate hydrolysis using the Molecular Devices kinetic microplate reader.[58,78] The IC_{50} (μ-plasmin−$KD1_{L17R}$-K_T concentration required for 50% decrease in Glu−Plg binding to the cell surface receptors) was determined by fitting the data to the following the IC_{50} four-parameter logistic equation from Halfman[79] given below

$$y = \frac{a}{1 + (x/\mathrm{IC}_{50})^s} \tag{3}$$

where y is the rate of S-2251 hydrolysis by plasmin generated from the Glu−Plg bound to the U937 cell receptors in the presence of a given concentration of $KD1_{L17R}$-K_T or $KD1_{L17R}$-V_T represented by x, a is the maximum rate of S-2251 hydrolysis in the absence of $KD1_{L17R}$-K_T or $KD1_{L17R}$-V_T, and s is the slope factor. Each point was weighted equally, and the data were fitted to eq 3 using the nonlinear regression analysis program GraFit from Erithcus Software. To obatian the K_d value for the interaction of $KD1_{L17R}$-K_T with Glu−Plg, we used the following equation, as described by Cheng and Prusoff[80] and further elaborated by Craig.[81]

$$K_{d\ (KD1_{L17R}\text{-}K_T)} = \frac{\mathrm{IC}_{50}}{1 + ([\mathrm{Glu{-}Plg}]/K_{d\ (\mathrm{Glu-Plg/cell\ surface\ receptors})})} \tag{4}$$

where [Glu−Plg] concentration employed was 2 μM (∼physiologic concentration).[9] To obtain the K_d ($KD1_{L17R}$-K_T) for Glu−Plg, we used a value of 1 μM for $K_{d\ (\mathrm{Glu-Plg/cell\ surface\ receptors})}$.[9,78,82]

Molecular Modeling. The crystal structures of μ-plasmin,[83] plasminogen kringle domain 1,[84] and wild-type KD1[69] were used as templates to model both the binary complex of $KD1_{L17R}$-K_T with plasmin kringle domain 1 and the ternary complex of $KD1_{L17R}$-K_T with the plasmin protease domain and kringle domain 1. The protocols for modeling these complexes have been described earlier.[66,85] Because the C-terminus residues are disordered in the wild-type KD1 crystal structure, we used the MODELLER program[86] to build this part of the KD1 molecule. The built models were further refined by energy minimization using the program CHARMM with the CHARMM19 force field[87] consisting of 50 steps of the steepest descent followed by 500 steps of adopted basis Newton−Raphson. Harmonic restraints of 10 kcal/mol/Å^2

were applied on the Cα atoms of the protein during the entire minimization.

RESULTS AND DISCUSSION

Proteolysis of $KD1_{L17R}$-V_T by IIa. In addition to the 58 residues corresponding to the BPTI-Kunitz domain, the 73-residue $KD1_{L17R}$-V_T construct contains additional nine residues at the N-terminus. The C-terminal tail residues (59EKVPKV64, BPTI numbering) in $KD1_{L17R}$-V_T contain two lysine residues.[66] We investigated whether incubation of $KD1_{L17R}$-V_T with higher concentrations of IIa, as compared to those used during the removal of His_6 tag, could cleave between the K60−V61 and/or between K63−V64 residues (59EK↓VPK↓V64). If so, then the resulting molecule(s), in addition to inhibiting the active site of plasmin, could also serve as a decoy receptor to attenuate pathological plasminogen activation. Incubation of $KD1_{L17R}$-V_T (1 mg/mL in TBS, pH 7.5) with IIa at a 1:50 enzyme/substrate molar ratio for 24 h at 37 °C resulted in the formation of a smaller molecular weight species referred to as $KD1_{L17R}$-K_T. SDS-PAGE data of KD_{1L17}-V_T and $KD1_{L17R}$-K_T are given in Figure 1. $KD1_{L17R}$-K_T was separated from IIa using Superdex-200 gel-filtration chromatography for further studies.

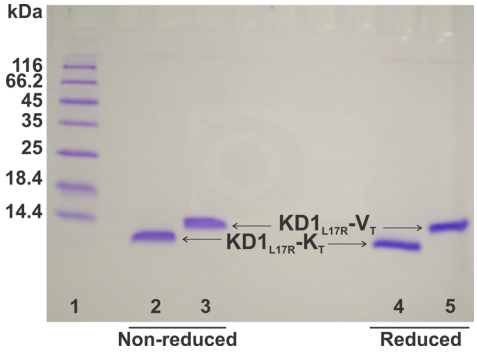

Figure 1. SDS-PAGE of $KD1_{L17R}$-V_T and $KD1_{L17R}$-K_T. Lane 1, mixture of reduced EZ-Run protein markers (Fisher BioReagents); lane 2, 5 μg of unreduced $KD1_{L17R}$-K_T; lane 3, 5 μg of unreduced $KD1_{L17R}$-V_T; lane 4, 5 μg of reduced $KD1_{L17R}$-K_T; and lane 5, 5 μg of reduced $KD1_{L17R}$-V_T. The concentration of acrylamide used was 15%.

The N-terminal sequence(s) of $KD1_{L17R}$-K_T is presented in Table 1, and the MALDI-TOF-ESI data are presented in Figure 2A. Combined analysis of the sequence(s) and the mass spectrometry data reveal that ∼80% of $KD1_{L17R}$-K_T has an N-terminal GNNAEI sequence and ∼20% has an N-terminal NAEI sequence; both species have the same C-terminal sequence, EKVPK. Amino acid sequence alignment of BPTI, $KD1_{L17R}$-V_T, and $KD1_{L17R}$-K_T is presented in Figure 2B. We interpret this to mean that IIa cleaved $KD1_{L17R}$-V_T between VPK↓V at the C-terminus; however, the hydrolysis at PT↓GN and GN↓NA at the N-terminus could be by IIa or conceivably by a contaminating protease(s). Notably, no cleavage was observed between EK↓VP at the C-terminus. Thus, $KD1_{L17R}$-K_T is homogeneous at the C-terminus, with ∼20% of the molecules lacking the first two amino acids at the N-terminus (Figure 2A,B).

Table 1. N-Terminal Sequence Analysis of IIa-Cleaved $KD1_{L17R}$-V_T[a]

cycle number	amino acid (pmol)	amino acid (pmol)
1	Gly (82.2)	Asn (19.2)
2	Asn (82.6)	Ala (21.5)
3	Asn (68.5)	Glu (16.5)
4	Ala (53.3)	Ile (14.7)
5	Glu (44.6)	X (Cys)
6	Ile (42.5)	Leu (12.8)
7	X (Cys)	Leu (11.9)
8	Leu (35.2)	Pro (10.8)

[a]There were two readable sequences one at the ∼80 pmol level and the other at the ∼20 pmol level. Note that the minor sequence is internal to the first sequence starting at cycle 3.

IIa cleaves Arg/Lys (P1 subsite)-×××× peptide bonds and has a strong preference for proline or a small hydrophobic residue at the P2 position.[88] Furthermore, a bulky or an acidic residue at the P2 position is strongly disfavored by IIa.[88,89] Accordingly, under the conditions of higher concentration of IIa used, cleavage between 62Pro-Lys↓Val64 (Figure 1S) of $KD1_{L17R}$-V_T is expected, whereas cleavage between 59Glu-Lys↓Val-Pro62 is disfavored (Figure 2B). Although threonine or asparagine at the P1 subsite is not preferred by IIa, its S1 pocket residue Asp189 can interact with Thr or Asn through a water molecule (Figure 1S). The proteolysis between Pro-Thr↓Gly-Asn or Gly-Asn↓Asn-Ala by IIa might also be facilitated by the presence of Pro or Gly at the P2 position (Figure 1S). As a result, we obtained a stable $KD1_{L17R}$-K_T protein that has an intact Kunitz domain and contains a C-terminal lysine.

$KD1_{L17R}$-K_T Binding to tPA and Glu−Plg. We used SPR to study the binding of $KD1_{L17R}$-K_T to immobilized tPA (Figure 3A) and Glu−Plg (Figure 3B). The k_{on} for binding of tPA to $KD1_{L17R}$-K_T was 0.91 ± 0.2 × 10^3 M^{-1} s^{-1}, k_{off} was 1.9 ± 0.3 × 10^{-4} s^{-1}, and K_d was 210 ± 20 nM. The k_{on} for binding of Glu−Plg to $KD1_{L17R}$-K_T was 1.1 ± 0.4 × 10^3 M^{-1} s^{-1}, k_{off} was 3.1 ± 0.8 × 10^{-4} s^{-1}, and K_d was 280 ± 30 nM. $KD1_{L17R}$-V_T showed negligible binding to tPA or Glu−Plg in SPR experiments, indicating that it is the C-terminal lysine in $KD1_{L17R}$-K_T that is necessary for this interaction.

Next, we modeled the complex of $KD1_{L17R}$-K_T with the kringle domain 1 of plasminogen. The C-terminal lysine binds in an analogous manner as εACA (Figure 3C). In addition, two other interactions were noted: one, a carboxylate of Glu59 of the inhibitor $KD1_{L17R}$-K_T makes a salt bridge with the guanidino group of Arg32 of plasminogen, and two, the carbonyl group of Lys60 of the inhibitor makes a hydrogen bond with the side chain of Arg70 of kringle domain 1 of plasminogen. These additional interactions could reflect the higher affinity of $KD1_{L17R}$-K_T for kringle domain 1 of plasminogen as compared to its affinity for εACA.[84,90] Although not investigated, on the basis of the SPR affinity data, similar interactions between tPA and $KD1_{L17R}$-K_T might exist.

Inhibition Profile of $KD1_{L17R}$-K_T. $KD1_{L17R}$-K_T inhibited plasmin (Figure 4) with a high affinity (K_i =1 ± 0.2 nM) very similar to $KD1_{L17R}$-V_T. Furthermore, both $KD1_{L17R}$-V_T[66] and $KD1_{L17R}$-K_T inhibited FXIa and *p*KLK with K_i > 10 μM (Figure 4). Moreover, $KD1_{L17R}$-V_T[66] or $KD1_{L17R}$-K_T (data not shown) did not inhibit IIa, activated protein C, tPA, uPA, or tissue kallikreins. Collectively, the data indicate that the Kuntiz domain in $KD1_{L17R}$-K_T is not altered and is fully functional.

Fibrinolysis Assay. These experiments were performed to compare the effectiveness of $KD1_{L17R}$-K_T, $KD1_{L17R}$-V_T, and εACA to inhibit tPA-induced plasma clot fibrinolysis. Addition of IIa to NPP caused fibrin formation, which is reflected by the increase in OD_{405} (curve 1, Figure 5A−C). Simultaneous

dx.doi.org/10.1021/bi401584b | Biochemistry 2014, 53, 505−517

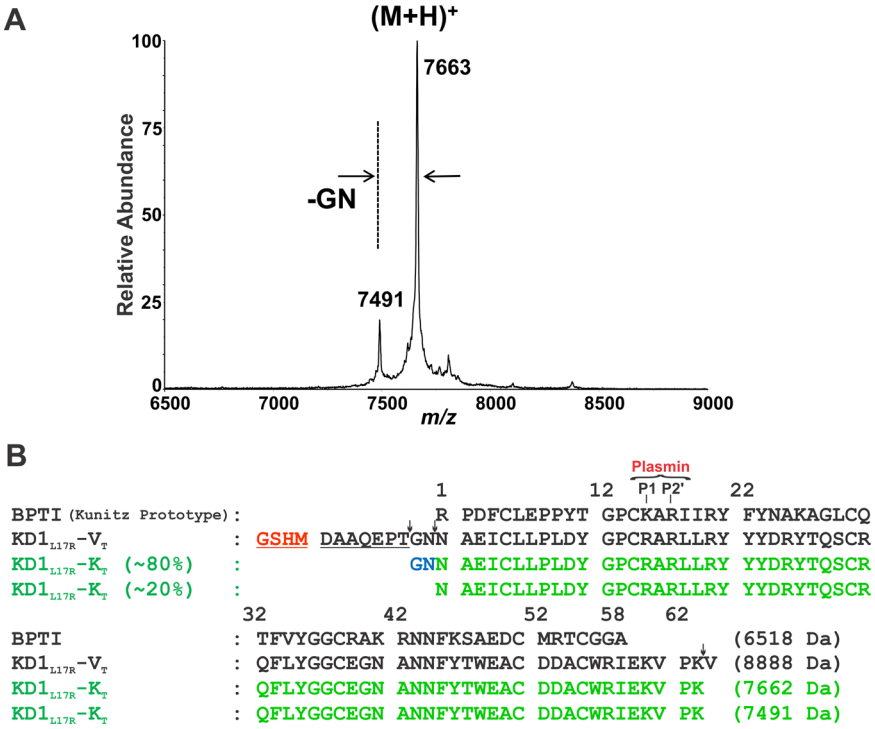

Figure 2. MALDI-TOF-ESI mass spectrometry data and amino acid sequence alignment of $KD1_{L17R}$-K_T with the starting molecule ($KD1_{L17R}$-V_T) and BPTI. (A) Mass spectrometry data of $KD1_{L17R}$-K_T obtained using an Applied Biosystems Voyager DE-STR. The spectra were calibrated; thus, the masses should be within 0.1% of the theoretical values. (B) Amino acid sequences of $KD1_{L17R}$-V_T and the two $KD1_{L17R}$-K_T species: one with N-terminus sequence Gly-Asn-Asn-Ala-Glu-Ile (~80%) and a second with N-terminus sequence Asn-Ala-Glu-Ile (~20%). Note that the minor sequence is internal to the major sequence starting at cycle 3 asparagine and that the calculated difference in MW between the two species is 171 Da; this is consistent with the mass spectrometry data shown in panel A. We infer that IIa or a contaminating protease cleaved the peptide bonds (shown by ↓) between amino acids Thr−Gly and Asn−Asn on the N-terminal side and between Lys−Val on the C-terminal side of $KD1_{L17R}$-V_T. The numbering system used is that of BPTI (prototype Kunitz inhibitor). The N-terminal Gly-Ser-His-Met sequence in $KD1_{L17R}$-V_T is derived from the IIa cleavage site introduced during cloning. The P1 and P2′ subsites recognized by plasmin are marked.

addition of tPA caused initial clot formation followed by dissolution of fibrin induced by tPA-mediated conversion of plasminogen to plasmin (curve 2, Figure 5A−C); the midpoint of fibrinolysis was between 6 to 7 min in each case. All three antifibrinolytic agents inhibited fibrinolysis in a dose-dependent manner. $KD1_{L17R}$-V_T increased the fibrinolysis midpoint to 22 min at 2 μM, to 29 min at 3 μM, and to 43 min at 5 μM, respectively (Figure 5A). In contrast, $KD1_{L17R}$-K_T increased the fibrinolysis midpoint to 27 min at 2 μM, to 37 min at 3 μM, and to >60 min at 5 μM, respectively (Figure 5A). Thus, at each concentration tested, $KD1_{L17R}$-K_T was more effective as an antifibrinolytic agent as compared to $KD1_{L17R}$-V_T. Because the active-site inhibition of plasmin by both $KD1_{L17R}$-V_T[66] and $KD1_{L17R}$-K_T is similar (Figure 4), the additional increased potency of $KD1_{L17R}$-K_T could be due to its binding to the kringle domains of tPA and/or plasminogen (Figure 3A,B). As a result, localized plasminogen activation at the fibrin clot might also be attenuated.

Higher concentrations of $KD1_{L17R}$-V_T or $KD1_{L17R}$-K_T were needed to inhibit fibrinolysis than those predicted from the K_i values for plasmin inhibition. A most likely explanation for these observations is that antifibrinolytic assay is a kinetic-based assay, whereas the equilibrium inhibition constant, K_i, was obtained upon prolonged incubation of the inhibitor with plasmin.

The antifibrinolytic activity of εACA is attributed to its binding to the kringle domains of tPA and plasminogen.[84,90] Therefore, we examined whether εACA could augment the fibrinolytic inhibition observed for $KD1_{L17R}$-V_T. These data are presented in Figure 5B. Equimolar additions of εACA to the $KD1_{L17R}$-V_T at 2, 3, or 5 μM had no observable effect on the extent of inhibition of plasma clot fibrinolysis. The most likely explanation for this observation is the low affinity (K_d ~ 10 μM)[84,90] of εACA for tPA or plasminogen as compared to the $KD1_{L17R}$-K_T (K_d ~ 0.2 to 0.3 μM; Figure 3). Consistent with these data, much higher concentrations of εACA were needed to inhibit plasma clot fibrinolysis in the absence of $KD1_{L17R}$-V_T (Figure 5C). Addition of εACA increased the clot lysis midpoint to 10 min at 0.1 mM, 19 min at 0.3 mM, and >60 min at 0.5 mM, respectively. Essentially no fibrinolysis was observed when the concentrations of εACA used were 1 or 5 mM.

Mouse Liver-Laceration Model. Because augmented fibrinolysis is an important cause of bleeding from small vessels in the mouse liver-laceration model,[91] we evaluated the efficacy of $KD1_{L17R}$-K_T in decreasing blood loss and compared it to the efficacy of εACA and $KD1_{L17R}$-V_T in this animal model. The dose of εACA, $KD1_{L17R}$-K_T, or $KD1_{L17R}$-V_T used is comparable to the dose used in a clinical setting. Although the half-life of each of these two antifibrinolytic agents is short (~2 h), a total duration of bleeding for 30 min should retain a sufficient level of each inhibitor for efficacy studies. The effects of the three antifibrinolytic agents on the quantity of blood loss are depicted in Figure 6. As compared to saline, the blood loss was reduced by ~74% by $KD1_{L17R}$-K_T (p = 0.001), ~50% by $KD1_{L17R}$-V_T (p = 0.002), and ~49% by εACA (p = 0.002). There was

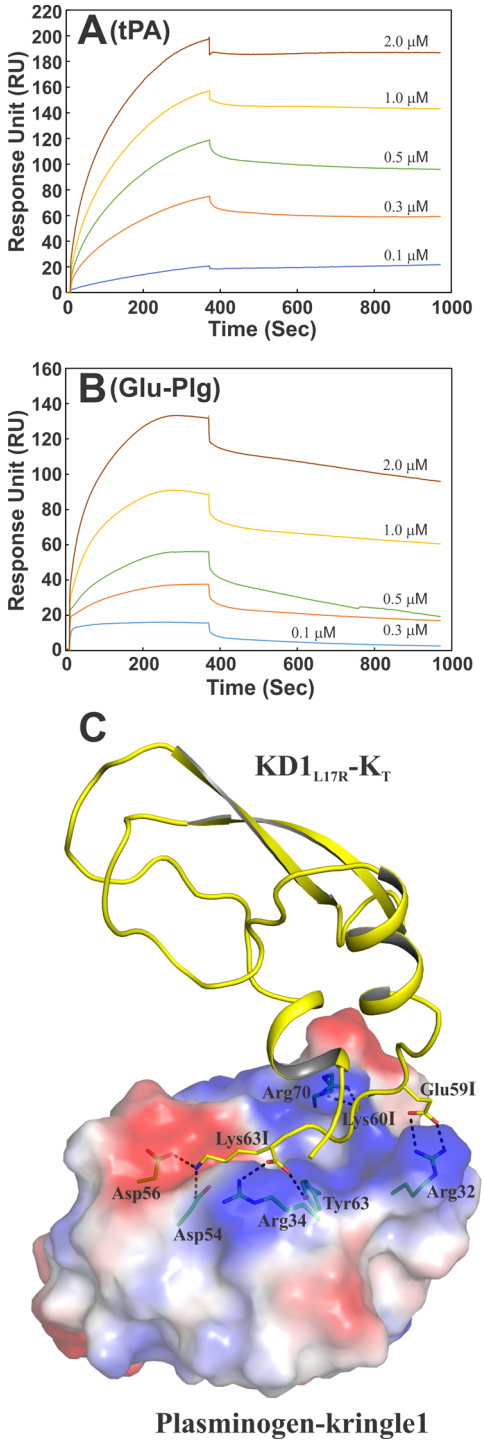

Figure 3. Interaction of $KD1_{L17R}$-K_T with tPA and Glu−Plg as measured by SPR. (A) tPA binding to $KD1_{L17R}$-K_T. tPA was coupled to the CM5 chip by the amine coupling method, and an immobilization level of 1193 response units (RU) was attained for the bound protein. Five concentrations (0.1−2 μM) of $KD1_{L17R}$-K_T were used, and 6 min association and 10 min dissociation times (flow rate of 10 μL/min) were employed. Details are provided in the Experimental Procedures. The RU value obtained with $KD1_{L17R}$-V_T at 1 μM was 16 instead of 155 with $KD1_{L17R}$-K_T. (B) Glu−Plg binding to $KD1_{L17R}$-K_T. Glu−Plg was coupled to the CM5 chip, and an immobilization level of 742 RU was attained for the bound protein. The concentrations of $KD1_{L17R}$-K_T used and the analyte association and dissociation protocols were the same as in panel A. The RU value obtained with $KD1_{L17R}$-V_T at 1 μM was 12 instead of 86 with $KD1_{L17R}$-K_T. (C) Modeled complex of $KD1_{L17R}$-K_T with plasminogen kringle domain 1. The electrostatic surface of the plasminogen kringle domain 1 and a cartoon representation of the $KD1_{L17R}$-K_T (yellow) are depicted. The residues that form hydrogen bonds and salt bridges (shown as dashed lines) between the kringle domain and $KD1_{L17R}$-K_T are shown in stick representation. The carbon atoms are shown in green for the kringle domain and yellow for $KD1_{L17R}$-K_T. Oxygen atoms are shown in red and nitrogen atoms, in blue. The $KD1_{L17R}$-K_T residues are labeled with the suffix I. In the electrostatic surface, blue represents positive, red represents negative, and white represents neutral charge.

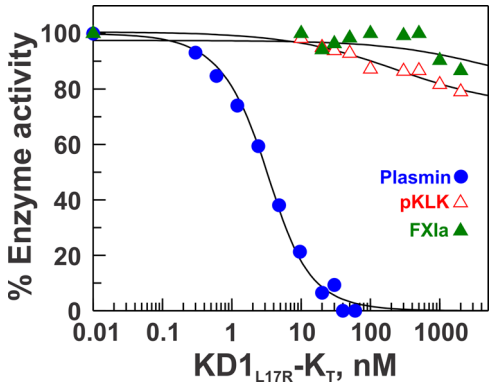

Figure 4. Determination of equilibrium inhibition constants (K_i) of $KD1_{L17R}$-K_T with plasmin, FXIa, and *p*KLK. The enzyme activity is expressed as the percent fractional activity (inhibited rate/uninhibited rate) at increasing inhibitor concentrations. The inhibition constants (K_i) were determined using eqs 1 and 2 as outlined in the Experimental Procedures. The concentration of plasmin used was 3 nM, whereas FXIa and *p*KLK were 1 nM each.

essentially no difference in the amount of blood loss between $KD1_{L17R}$-V_T- and εACA-treated animals. Of significance is the observation that $KD1_{L17R}$-K_T is more effective than $KD1_{L17R}$-V_T ($p < 0.05$) or εACA ($p < 0.05$) in inhibiting plasmin-induced fibrinolysis and blood loss in this animal model.

Unexpectedly, our present data with $KD1_{L17R}$-K_T is not statistically different from the previous data obtained with KD1-L17R, which was presumed to have Val at the C-terminus.[66] To address this discrepancy, we performed SDS-PAGE, mass spectrometry, and N-terminal sequence analysis on the actual KD1-L17R preparation used in the previous animal studies. These data are presented in the Supporting Information Figure 2S. Evidently, the KD1-L17R previously used is composed of 76 amino acids with an N-terminal sequence of Gly-Ser-His and a C-terminal sequence of Val-Pro-Lys (instead of Pro-Lys-Val). Thus, our present data with $KD1_{L17R}$-K_T and the previous data with KD1-L17R (C-terminal lysine) support a concept that these molecular species have improved efficacy than the $KD1_{L17R}$-V_T in preventing blood loss in the mouse liver-laceration model.

Importantly, 4 of the 16 animals (one out of four each day) treated with εACA depicted generalized seizures shortly after injection of the drug. During surgery, these animals had unilateral or bilateral clonic movements on 3−4.5% isoflurane. Abnormal movements were not observed during the induction of anesthesia, but rather 15−20 min after the onset of surgery. Seizures appeared as repetitive clonic movements of one or more extremities while the animal remained unresponsive

dx.doi.org/10.1021/bi401584b | *Biochemistry* 2014, 53, 505−517

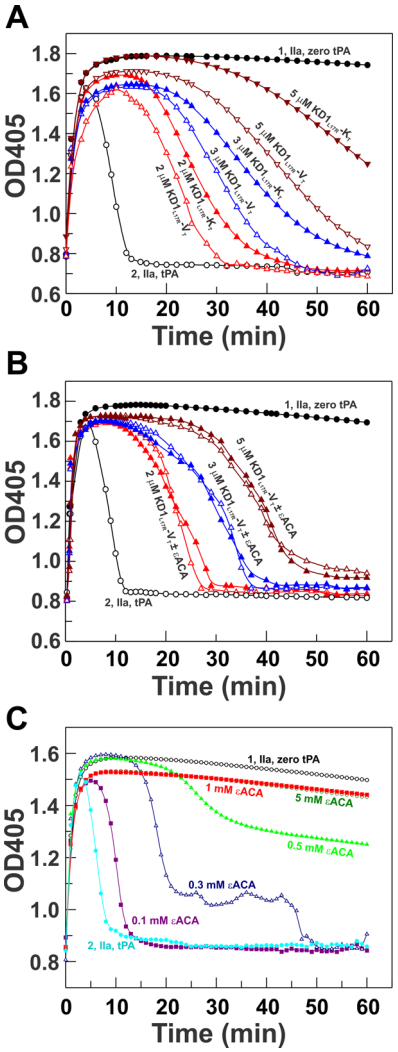

Figure 5. Effect of $KD1_{L17R}$-V_T, $KD1_{L17R}$-K_T, and εACA on fibrinolysis in human NPP. IIa was added to NPP to initiate clot formation, which is associated with an increase in optical density at 405 nm (curve 1 in panels A, B, and C). Simultaneous addition of tPA converted plasminogen to plasmin, which dissolved the fibrin clot completely within ~10 min, as indicated by an initial increase followed by a decrease in OD_{405} (curve 2 in panels A, B, and C). (A) Inhibition of fibrinolysis by $KD1_{L17R}$-V_T and $KD1_{L17R}$-K_T. $KD1_{L17R}$-V_T: 2 (red open triangles), 3 (blue open triangles), and 5 μM (brown open triangles). $KD1_{L17R}$-K_T: 2 (red closed triangles), 3 (blue closed triangles), and 5 μM (brown closed triangles). In each case, IIa was used to initiate clotting and tPA to initiate fibrinolysis. (B) Effect of εACA on the inhibition of fibrinolysis by $KD1_{L17R}$-V_T. $KD1_{L17R}$-V_T: 2 (red open triangles), 3 (blue open triangles), and 5 μM (brown open triangles). $KD1_{L17R}$-K_T plus equimolar εACA: 2 (red closed triangles), 3 (blue closed triangles), and 5 μM (brown closed triangles). As in panel A, in each case, IIa was used to initiate clotting and tPA was used to initiate fibrinolysis. (C) Inhibition of fibrinolysis by εACA alone: 0.1 (magenta closed squares), 0.3 (blue open triangles), 0.5 (green closed triangles), 1.0 (red closed squares) and 5 mM (green open circles). As in panels A and B, in each case, IIa was used to initiate clotting and tPA was used to initiate fibrinolysis.

under anesthesia. Animals were not observed to have any tonic movements. Convulsion and seizures have been previously observed in animals given εACA or TE and represent a major side effect of these drugs as antifibrinolytic agents.[92,93]

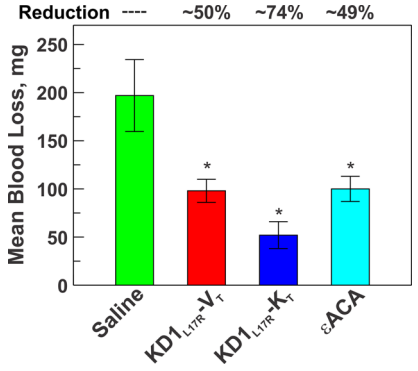

Figure 6. Effect of $KD1_{L17R}$-V_T, $KD1_{L17R}$-K_T, and εACA in a mouse liver-laceration bleeding model. Animals were treated with saline, $KD1_{L17R}$-V_T, $KD1_{L17R}$-K_T, or εACA by intravenous injection. A 5 mm transverse incision was made on the left lobe of the liver. All blood oozing from the incision site was collected for a total duration of 30 min. Total blood loss was compared between different groups. Data are presented as the mean ± SE of 10 animals each for saline, $KD1_{L17R}$-V_T, and $KD1_{L17R}$-K_T and 16 animals for εACA. Probability p values between different groups were as follows: saline vs $KD1_{L17R}$-V_T, 0.002; saline vs $KD1_{L17R}$-K_T, 0.001; saline vs εACA, 0.002; $KD1_{L17R}$-K_T vs $KD1_{L17R}$-V_T, < 0.05; and $KD1_{L17R}$-K_T vs εACA, < 0.05. *, p value < 0.01 compared with saline control.

Our observation is also consistent with the recent findings that εACA[39,40,94] or TE[39,94,95] cause seizures and convulsions in a significant number of patients. The εACA and TE concentrations associated with human seizures inhibit glycine receptors and could be the mechanism for the observed side effects.[93] In contrast, aprotinin did not inhibit the function of the glycine receptors.[93] These observations are consistent with our animal data, where we did not observe seizures in animals treated with either $KD1_{L17R}$-V_T or $KD1_{L17R}$-K_T. Furthermore, the use of εACA, TE, and aprotinin is associated with renal dysfunction/failure,[36−39,94] whereas two KD1 molecules (with Arg15 → Lys or Leu17 → Arg) of TFPI-2 did not cause renal toxicity in mouse[66] or rat.[96] Thus, $KD1_{L17R}$-K_T could be a preferred agent in attenuating fibrinolysis in vivo.

Effects of μ-Plasmin−$KD1_{L17R}$-K_T on Glu−Plg Binding to PMA-Stimulated Nonadherent U937 Cells. A majority of the cell surface receptors for plasminogen have lysine as their C-terminal residue.[82] We examined whether $KD1_{L17R}$-K_T (and not $KD1_{L17R}$-V_T) binds to the kringle domain(s) of Glu−Plg and prevents its binding to the U937 cell surface receptors. First, we prepared μ-plasmin−$KD1_{L17R}$-V_T and μ-plasmin−$KD1_{L17R}$-K_T to block the Kuntiz domain function. The SDS-PAGE of the Superdex-200 gel-purified complexes of μ-plasmin−$KD1_{L17R}$-V_T and μ-plasmin−$KD1_{L17R}$-K_T are shown in the inset of Figure 7A. Next, we incubated PMA-stimulated U937 cells with Glu−Plg containing varying concentrations of μ-plasmin−$KD1_{L17R}$-V_T or μ-plasmin−$KD1_{L17R}$-K_T (given in legend to Figure 7A). The increasing concentrations of μ-plasmin−$KD1_{L17R}$-K_T (but not of μ-plasmin−$KD1_{L17R}$-V_T) inhibited Glu−Plg binding to the cell surface receptors deduced from the S-2251 hydrolysis data shown in Figure 7A. The percent reduction in plasmin generation by the purified μ-plasmin−$KD1_{L17R}$-K_T or μ-plasmin−$KD1_{L17R}$-V_T is presented in Figure 7B. We interpret these data to mean that the μ-plasmin−$KD1_{L17R}$-K_T complex interferes with Glu−Plg binding to the PMA-stimulated U937 cells. Using eqs 3 and 4, a K_d value for the interaction of $KD1_{L17R}$-K_T with Glu−Plg was

dx.doi.org/10.1021/bi401584b | Biochemistry 2014, 53, 505−517

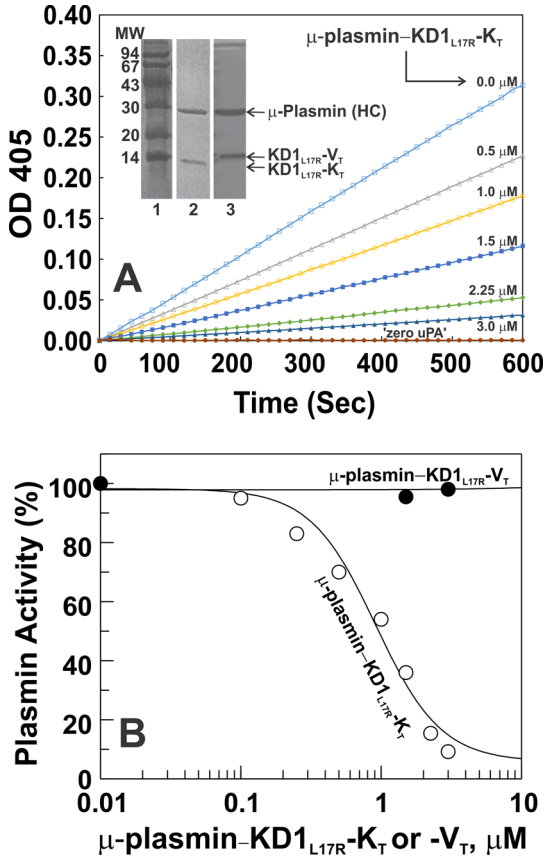

Figure 7. Inhibition of Glu–Plg binding to PMA-stimulated nonadherent U937 cells by μ-plasmin–$KD1_{L17R}$-K_T. (A) Proteolytic activity of plasmin generated on the U937 cell surface. PMA-stimulated U937 cells (200 μL, 10^6 cells/mL) in HBS/BSA, pH 7.5, were incubated at 37 °C for 1 h with 2 μM Glu–Plg containing various concentrations of μ-plasmin–$KD1_{L17R}$-K_T (ranging from 0 to 3 μM) or μ-plasmin–$KD1_{L17R}$-V_T (2 and 4 μM). The cells were washed, and the cell-surface-bound Glu–Plg was activated with 10 nM uPA for 20 min at 37 °C. The samples were diluted 10-fold, and the plasmin formed was measured by S-2251 synthetic-substrate hydrolysis (OD_{405}) as outlined in the Experimental Procedures. μ-Plasmin–$KD1_{L17R}$-K_T reduced the plasmin formed in a dose-dependent manner, whereas μ-plasmin–$KD1_{L17R}$-V_T had no effect (see panel B). Inset, reduced SDS-PAGE (15% acrylamide) of the size-exclusion gel-purified μ-plasmin–$KD1_{L17R}$-K_T and μ-plasmin–$KD1_{L17R}$-V_T. The μ-plasmin expressed consists of residues 542–791 cleaved between R561 (R15 in chymotrypsin numbering) and V562 (V16 in chymotrypsin numbering). (The chymotrypsin amino acid numbering system is used for the protease domain of plasmin and IIa. Residue 195 in chymotrypsin numbering corresponds to 741 in plasmin and 525 in IIa. Similarly, residue 189 in chymotrypsin numbering corresponds to 735 in plasmin and 519 in IIa.) The heavy chain (HC) consists of residues 562–791 and the light chain consists of 20 residues of 542–561 and is not seen on the gel. Lane 1, MW markers; lane 2, μ-plasmin–$KD1_{L17R}$-K_T complex; lane 3, μ-plasmin–$KD1_{L17R}$-V_T complex. (B) Percent reduction of plasmin generation by purified μ-plasmin–$KD1_{L17R}$-K_T and μ-plasmin–$KD1_{L17R}$-V_T. The plasmin activity is expressed as percent fractional activity (inhibited rate/uninhibited rate) at increasing inhibitor concentrations. (○, μ-plasmin–$KD1_{L17R}$-K_T; and ●, μ-plasmin–$KD1_{L17R}$-V_T.)

calculated to be ~300 nM, a value consistent with the value (~280 nM) obtained from the SPR data (Figure 3B).

The data presented in Figure 7 support a conclusion that a single molecule of $KD1_{L17R}$-K_T can bind simultaneously to the kringle domain of plasminogen/plasmin as well as to the active site of plasmin. A modeled ternary complex of $KD1_{L17R}$-K_T with the plasmin protease domain and the plasminogen/plasmin kringle domain 1 is depicted in Figure 8. The $KD1_{L17R}$-K_T via its P5–P5′ residues interacts with the active site of plasmin, a typical mode of Kunitz domain binding to a serine protease domain. Similarly, the interactions of the C-terminal lysine of $KD1_{L17R}$-K_T with the kringle domain 1 of plasminogen/plasmin are analogous to the lysine analogues εACA or TE. However, as compared to the lysine analogues, $KD1_{L17R}$-K_T has additional contacts with the kringle domain 1 of plasminogen/plasmin that makes the binding considerably stronger (Figure 8).

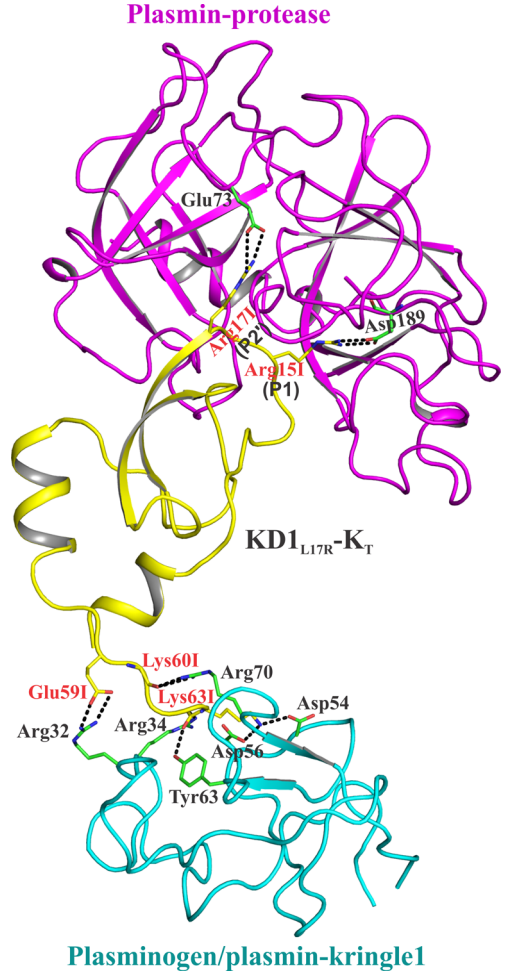

Figure 8. Modeled ternary complex of $KD1_{L17R}$-K_T with the protease domain of plasmin and the kringle domain 1 of plasminogen/plasmin. A cartoon representation of the $KD1_{L17R}$-K_T (yellow) bound to the plasmin protease domain (magenta) and plasminogen/plasmin kringle domain 1 (cyan) is shown. The $KD1_{L17R}$-K_T C-terminal residues that make hydrogen bonds and salt bridges with residues of the kringle domain 1 are shown in stick representation. Similarly, residues Arg15 and Arg17 of the Kunitz domain that interact with residue Asp189 and Glu73 (chymotrypsin numbering) of the plasmin protease domain are shown in stick representation. The carbon atoms in plasminogen/plasmin are in green, whereas they are yellow in $KD1_{L17R}$-K_T. Oxygen and nitrogen atoms are in red and blue, respectively. The $KD1_{L17R}$-K_T residues are labeled with the suffix I.

CONCLUSIONS

Previously, we demonstrated that changing residue Leu17 (BPTI/aprotinin numbering) to Arg in KD1 (73-residue

dx.doi.org/10.1021/bi401584b | Biochemistry 2014, 53, 505–517

construct $KD1_{L17R}$-V_T) of TFPI-2 abolishes its anticoagulant functions and enhances its plasmin inhibition.[66] $KD1_{L17R}$-V_T has nine residues at the N-terminus that are not part of the Kunitz domain. Furthermore, it has valine at the C-terminus, which would prevent its binding to the kringle domains of plasminogen/plasmin. In this article, we obtained a $KD1_{L17R}$-K_T molecule that lacks the N-terminal residues and primarily contains the Kunitz domain with a C-terminal lysine. As expected, both $KD1_{L17R}$-V_T and $KD1_{L17R}$-K_T inhibit plasmin with the same affinity. However, in contrast to $KD1_{L17R}$-V_T, $KD1_{L17R}$-K_T binds to the kringle domain(s) of tPA and plasminogen via its C-terminal lysine residue. Consequently, $KD1_{L17R}$-K_T (and not $KD1_{L17R}$-V_T) inhibits Glu−Plg binding to U937 cells and therefore serves as a decoy plasminogen receptor. Furthermore, $KD1_{L17R}$-K_T inhibits tPA-induced plasma clot fibrinolysis more potently than $KD1_{L17R}$-V_T (Figure 5A). These data represent a dual function of $KD1_{L17R}$-K_T: one, it attenuates tPA and plasminogen binding to the exposed C-terminal lysine residues in the fibrin, which reduces plasmin formation, and two, it inhibits the active site of the generated plasmin. Thus, $KD1_{L17R}$-K_T is a superior antifibrinolytic agent in each of the in vitro experiment performed.

The efficacy of $KD1_{L17R}$-K_T in reducing blood loss in the mouse liver-laceration model is also improved ($p < 0.05$) as compared to $KD1_{L17R}$-V_T (Figure 6). Importantly, in the mice treated with εACA, we observed generalized seizures in 25% of the animals. We did not observe such adverse effects with $KD1_{L17R}$-K_T. With its dual function, $KD1_{L17R}$-K_T could be a useful agent in situations where the fybrinolytic system needs to be significantly weakened to prevent blood loss as well as to prevent uPA-mediated activation of plasminogen on cell surfaces.

■ ASSOCIATED CONTENT

Ⓢ Supporting Information

Modeled molecular interactions between the S1 pocket residue Asp189 of thrombin (IIa) and the P1 residue (recognized by IIa) of $KD1_{L17R}$-V_T at the three observed cleavage sites and MALDI-TOF mass spectrometry data including the amino acid sequence of the KD1-L17R employed in our previous study[66] in the mouse liver-laceration bleeding model. This material is available free of charge via the Internet at http://pubs.acs.org.

■ AUTHOR INFORMATION

Corresponding Author

*Tel: 01-310-825-5622; Fax: 01-310-825-5972; E-mail: pbajaj@mednet.ucla.edu.

Author Contributions

#These authors contributed equally to this work

Funding

Supported by National Heart, Lung, and Blood Institute grants R01HL36365 to S.P.B. and R21HL89961 to M.S.B. as well as by U.S. National Institutes of Health grants R01GM103479 and S10RR028893 to J.A.L.

Notes

The authors declare no competing financial interest.

■ DEDICATION

We dedicate this paper to the memory of Walter Kisiel, Ph.D., who made seminal contributions to the field of TFPI-2.

■ ABBREVIATIONS USED

BPTI, bovine pancreatic trypsin inhibitor; BSA, bovine serum albumin; εACA, ε-aminocaproic acid; ECM, extracellular matrix; FXIa, factor XIa; Glu−Plg, Glu-plasminogen; HBS/BSA, 50 mM Hepes containing 100 mM NaCl, 0.1 mg/mL BSA, pH 7.5; HBS-P, 20 mM Hepes containing 100 mM NaCl and 0.005% (v/v) P20, pH 7.4; IIa, thrombin; IPTG, isopropyl thiogalactopyranoside; KD1, Kunitz domain 1; MMP, matrix metalloproteases; NPP, normal pooled plasma; PAI-1, plasminogen activator inhibitor-1; PAI-2, plasminogen activator inhibitor-2; PMA, 12-*O*-tetradecanoylphorbol-13-acetate; S-2251, H-D-Val-Leu-Lys-*p*-nitroanilide; S-2366, pyroGlu-Pro-Arg-*p*-nitroanilide; SPR, surface plasmon resonance; TBS, 50 mM Tris-HCl containing 100 mM NaCl, pH 7.5; TBS/BSA, TBS containing 0.1 mg/mL of BSA; TE, tranexamic acid; TFPI-2, tissue factor pathway inhibitor-2; tPA, tissue plasminogen activator; pKLK, plasma kallikrein; uPA, urokinase plasminogen activator

■ REFERENCES

(1) Petersen, T. E., Martzen, M. R., Ichinose, A., and Davie, E. W. (1990) Characterization of the gene for human plasminogen, a key proenzyme in the fibrinolytic system. *J. Biol. Chem. 265*, 6104−6111.

(2) Zhang, L., Seiffert, D., Fowler, B. J., Jenkins, G. R., Thinnes, T. C., Loskutoff, D. J., Parmer, R. J., and Miles, L. A. (2002) Plasminogen has a broad extrahepatic distributions. *Thromb. Haemostasis 87*, 493−501.

(3) Bohmfalk, J. F., and Fuller, G. M. (1980) Plasminogen is synthesized by primary cultures of rat hepatocytes. *Science 209*, 408−410.

(4) Saito, H., Hamilton, S. M., Tavill, A. S., Louis, L., and Ratnoff, O. D. (1980) Production and release of plasminogen by isolated perfused rat-liver. *Proc. Natl. Acad. Sci. U.S.A. 77*, 6837−6840.

(5) Miles, L. A., Castellino, F. J., and Gong, Y. (2003) Critical role for conversion of glu-plasminogen to Lys-plasminogen for optimal stimulation of plasminogen activation on cell surfaces. *Trends Cardiovasc. Med. 13*, 21−30.

(6) Cockell, C. S., Marshall, J. M., Dawson, K. M., Cederholm-Williams, S. A., and Ponting, C. P. (1998) Evidence that the conformation of unliganded human plasminogen is maintained via an intramolecular interaction between the lysine-binding site of kringle 5 and the N-terminal peptide. *Biochem. J. 333*, 99−105.

(7) Law, R. H. P., Caradoc-Davies, T., Cowieson, N., Horvath, A. J., Quek, A. J., Encarnacao, J. A., Steer, D., Cowan, A., Zhang, Q. W., Lu, B. G. C., Pike, R. N., Smith, A. I., Coughlin, P. B., and Whisstock, J. C. (2012) The X-ray crystal structure of full-length human plasminogen. *Cell Rep. 1*, 185−190.

(8) Violand, B. N., and Castellino, F. J. (1976) Mechanism of urokinase-catalyzed activation of human plasminogen. *J. Biol. Chem. 251*, 3906−3912.

(9) Castellino, F. J., and Ploplis, V. A. (2005) Structure and function of the plasminogen/plasmin system. *Thromb. Haemostasis 93*, 647−654.

(10) Ellis, V., Behrendt, N., and Dano, K. (1991) Plasminogen activation by receptor-bound urokinase. A kinetic-study with both cell-associated and isolated receptor. *J. Biol. Chem. 266*, 12752−12758.

(11) Urano, T., Deserrano, V. S., Gaffney, P. J., and Castellino, F. J. (1988) Effectors of the activation of human [glu]plasminogen by human-tissue plasminogen-activator. *Biochemistry 27*, 6522−6528.

(12) Violand, B. N., Sodetz, J. M., and Castellino, F. J. (1975) Effect of ε-amino caproic acid on gross conformation of plasminogen and plasmin. *Arch. Biochem. Biophys. 170*, 300−305.

(13) Markus, G., Evers, J. L., and Hobika, G. H. (1978) Comparison of some properties of native (glu) and modified (lys) human plasminogen. *J. Biol. Chem. 253*, 733−739.

(14) Claeys, H., and Vermylen, J. (1974) Physicochemical and proenzyme properties of NH_2-terminal glutamic-acid and NH_2-

terminal lysine human plasminogen: Influence of 6-aminohexanoic acid. *Biochim. Biophys. Acta 342*, 351−359.
(15) Fredenburgh, J. C., and Nesheim, M. E. (1992) Lys-plasminogen is a significant intermediate in the activation of glu-plasminogen during fibrinolysis invitro. *J. Biol. Chem. 267*, 26150−26156.
(16) Kruithof, E. K. O., Tranthang, C., Ransijn, A., and Bachmann, F. (1984) Demonstration of a fast-acting inhibitor of plasminogen activators in human-plasma. *Blood 64*, 907−913.
(17) Åstedt, B., Lecander, I., and Ny, T. (1987) The placental type plasminogen activator inhibitor, PAI 2. *Fibrinolysis 1*, 203−208.
(18) Sprengers, E. D., and Kluft, C. (1987) Plasminogen-activator inhibitors. *Blood 69*, 381−387.
(19) Collen, D., and Wiman, B. (1978) Fast-acting plasmin inhibitor in human-plasma. *Blood 51*, 563−569.
(20) Hall, S. W., Humphries, J. E., and Gonias, S. L. (1991) Inhibition of cell-surface receptor-bound plasmin by alpha-2-antiplasmin and alpha-2-macroglobulin. *J. Biol. Chem. 266*, 12329−12336.
(21) Collen, D. (2001) Ham-Wasserman lecture: Role of the plasminogen system in fibrin-homeostasis and tissue remodeling. *Hematology*, 1−9.
(22) Camiolo, S. M., Thorsen, S., and Astrup, T. (1971) Fibrinogenolysis and fibrinolysis with tissue plasminogen activator, urokinase, streptokinase-activated human globulin, and plasmin. *Proc. Soc. Exp. Biol. Med. 138*, 277−280.
(23) Pennica, D., Holmes, W. E., Kohr, W. J., Harkins, R. N., Vehar, G. A., Ward, C. A., Bennett, W. F., Yelverton, E., Seeburg, P. H., Heyneker, H. L., Goeddel, D. V., and Collen, D. (1983) Cloning and expression of human tissue-type plasminogen-activator cDNA in Escherichia coli. *Nature 301*, 214−221.
(24) Banyai, L., Varadi, A., and Patthy, L. (1983) Common evolutionary origin of the fibrin-binding structures of fibronectin and tissue-type plasminogen-activator. *FEBS Lett. 163*, 37−41.
(25) Devries, C., Veerman, H., and Pannekoek, H. (1989) Identification of the domains of tissue-type plasminogen-activator involved in the augmented binding to fibrin after limited digestion with plasmin. *J. Biol. Chem. 264*, 12604−12610.
(26) Vanzonneveld, A. J., Veerman, H., and Pannekoek, H. (1986) On the interaction of the finger and the kringle-2 domain of tissue-type plasminogen-activator with fibrin. Inhibition of kringle-2 binding to fibrin by epsilon-amino caproic acid. *J. Biol. Chem. 261*, 14214−14218.
(27) Devries, C., Veerman, H., Koornneef, E., and Pannekoek, H. (1990) Tissue-type plasminogen-activator and its substrate glu-plasminogen share common binding-sites in limited plasmin-digested fibrin. *J. Biol. Chem. 265*, 13547−13552.
(28) Weisel, J. W., and Dempfle, C. H. (2012) Fibrinogen structure and function, in *Hemostasis and Thrombosis* (Marder, V. J., Aird, W. C., Bennett, J. S., Schulman, S., and White, G. C., Eds.) 6th ed., pp 254−271, Lippincott Williams & Wilkins, Philadelphia, PA.
(29) Satkurunath, G., and Royston, D. (2008) Hemostatic drugs in trauma and orthopaedic practice. *Int. Trauma Care 18*, 24−28.
(30) Hartmann, M., Sucker, C., Boehm, O., Koch, A., Loer, S., and Zacharowski, K. (2006) Effects of cardiac surgery on hemostasis. *Transfus. Med. Rev. 20*, 230−241.
(31) Dhir, A. (2013) Antifibrinolytics in cardiac surgery. *Ann. Card. Anaesth. 16*, 117−125.
(32) Sauaia, A., Moore, F. A., Moore, E. E., Moser, K. S., Brennan, R., Read, R. A., and Pons, P. T. (1995) Epidemiology of trauma deaths: A reassessment. *J. Trauma 38*, 185−193.
(33) Levy, J. H. (2006) Aprotinin is useful as a hemostatic agent in cardiopulmonary surgery: Yes. *J. Thromb. Haemostasis 4*, 1875−1878.
(34) Levi, M., Cromheecke, M. E., de Jonge, E., Prins, M. H., de Mol, B. J. M., Briet, E., and Buller, H. R. (1999) Pharmacological strategies to decrease excessive blood loss in cardiac surgery: A meta-analysis of clinically relevant endpoints. *Lancet 354*, 1940−1947.
(35) Royston, D., Van Haaften, N., and De Vooght, P. (2007) Aprotinin; friend or foe? A review of recent medical literature. *Eur. J. Anaesthesiol. 24*, 6−14.
(36) Mangano, D. T., Tudor, I. C., Dietzel, C., Is, M. S. P., and Fdn, I. R. E. (2006) The risk associated with aprotinin in cardiac surgery. *N. Engl. J. Med. 354*, 353−365.
(37) Immer, F. F., Jent, P., Englberger, L., Stalder, M., Gygax, E., Carrel, T. P., and Tevaearai, H. T. (2008) Aprotinin in cardiac surgery: A different point of view. *Heart Surg. Forum 11*, E9−E12.
(38) Beierlein, W., Scheule, A. M., Dietrich, W., and Ziemer, G. (2005) Forty years of clinical aprotinin use: A review of 124 hypersensitivity reactions. *Ann. Thorac. Surg. 79*, 741−748.
(39) Martin, K., Knorr, J., Breuer, T., Gertler, R., MacGuill, M., Lange, R., Tassani, P., and Wiesner, G. (2011) Seizures after open heart surgery: Comparison of epsilon-aminocaproic acid and tranexamic acid. *J. Cardiothorac. Vasc. Anesth. 25*, 20−25.
(40) Rabinovici, R., Heyman, A., Kluger, Y., and Shinar, E. (1989) Convulsions induced by aminocaproic acid infusion. *DICP, Ann. Pharmacother. 23*, 780−781.
(41) Salonen, E. M., Zitting, A., and Vaheri, A. (1984) Laminin interacts with plasminogen and its tissue-type activator. *FEBS Lett. 172*, 29−32.
(42) Silverstein, R. L., Leung, L. L. K., Harpel, P. C., and Nachman, R. L. (1984) Complex-formation of platelet thrombospondin with plasminogen. Modulation of activation by tissue activator. *J. Clin. Invest. 74*, 1625−1633.
(43) Salonen, E. M., Saksela, O., Vartio, T., Vaheri, A., Nielsen, L. S., and Zeuthen, J. (1985) Plasminogen and tissue-type plasminogen-activator bind to immobilized fibronectin. *J. Biol. Chem. 260*, 2302−2307.
(44) Lijnen, H. R., Van Hoef, B., Lupu, F., Moons, L., Carmeliet, P., and Collen, D. (1998) Function of the plasminogen/plasmin and matrix metalloproteinase systems after vascular injury in mice with targeted inactivation of fibrinolytic system genes. *Arterioscler., Thromb., Vasc. Biol. 18*, 1035−1045.
(45) Bonnefoy, A., and Legrand, C. (2000) Proteolysis of subendothelial adhesive glycoproteins (fibronectin, thrombospondin, and von Willebrand factor) by plasmin, leukocyte cathepsin G, and elastase. *Thromb. Res. 98*, 323−332.
(46) Lijnen, H. R. (2000) Molecular interactions between the plasminogen/plasmin and matrix metalloproteinase systems. *Fibrinolysis Proteolysis 14*, 175−181.
(47) Plow, E. F., Herren, T., Redlitz, A., Miles, L. A., and Hooverplow, J. L. (1995) The cell biology of the plasminogen system. *FASEB J. 9*, 939−945.
(48) He, C. S., Wilhelm, S. M., Pentland, A. P., Marmer, B. L., Grant, G. A., Eisen, A. Z., and Goldberg, G. I. (1989) Tissue cooperation in a proteolytic cascade activating human interstitial collagenase. *Proc. Natl. Acad. Sci. U.S.A. 86*, 2632−2636.
(49) Okada, Y., Gonoji, Y., Naka, K., Tomita, K., Nakanishi, I., Iwata, K., Yamashita, K., and Hayakawa, T. (1992) Matrix metalloproteinase-9 (92-kDa gelatinase/type IV collagenase) from HT 1080 human fibrosarcoma cells. Purification and activation of the precursor and enzymatic-properties. *J. Biol. Chem. 267*, 21712−21719.
(50) Holliday, L. S., Welgus, H. G., Fliszar, C. J., Veith, G. M., Jeffrey, J. J., and Gluck, S. L. (1997) Initiation of osteoclast bone resorption by interstitial collagenase. *J. Biol. Chem. 272*, 22053−22058.
(51) Gong, Y. Q., Hart, E., Shchurin, A., and Hoover-Plow, J. (2008) Inflammatory macrophage migration requires MMP-9 activation by plasminogen in mice. *J. Clin. Invest. 118*, 3012−3024.
(52) Lee, S., Jilani, S. M., Nikolova, G. V., Carpizo, D., and Iruela-Arispe, M. L. (2005) Processing of VEGF-A by matrix metalloproteinases regulates bioavailability and vascular patterning in tumors. *J. Cell. Biol. 169*, 681−691.
(53) McColl, B. K., Baldwin, M. E., Roufail, S., Freeman, C., Moritz, R. L., Simpson, R. J., Alitalo, K., Stacker, S. A., and Achen, M. G. (2003) Plasmin activates the lymphangiogenic growth factors VEGF-C and VEGF-D. *J. Exp. Med. 198*, 863−868.

(54) Falcone, D. J., Mccaffrey, T. A., Haimovitzfriedman, A., Vergilio, J. A., and Nicholson, A. C. (1993) Macrophage and foam cell release of matrix-bound growth-factors. Role of plasminogen activation. *J. Biol. Chem. 268*, 11951−11958.
(55) Syrovets, T., Lunov, O., and Simmet, T. (2012) Plasmin as a proinflammatory cell activator. *J. Leukocyte Biol. 92*, 509−519.
(56) Miles, L. A., Dahlberg, C. M., and Plow, E. F. (1988) The cell-binding domains of plasminogen and their function in plasma. *J. Biol. Chem. 263*, 11928−11934.
(57) Miles, L. A., Dahlberg, C. M., Plescia, J., Felez, J., Kato, K., and Plow, E. F. (1991) Role of cell-surface lysines in plasminogen binding to cells: Identification of alpha-enolase as a candidate plasminogen receptor. *Biochemistry 30*, 1682−1691.
(58) Andronicos, N. M., Chen, E. I., Baik, N., Bai, H., Parmer, C. M., Kiosses, W. B., Kamps, M. P., Yates, J. R., Parmer, R. J., and Miles, L. A. (2010) Proteomics-based discovery of a novel, structurally unique, and developmentally regulated plasminogen receptor, Plg-R-KT, a major regulator of cell surface plasminogen activation. *Blood 115*, 1319−1330.
(59) Liotta, L. A., Goldfarb, R. H., Brundage, R., Siegal, G. P., Terranova, V., and Garbisa, S. (1981) Effect of plasminogen-activator (urokinase), plasmin, and thrombin on glycoprotein and collagenous components of basement-membrane. *Cancer Res. 41*, 4629−4636.
(60) Festuccia, C., Dolo, V., Guerra, F., Violini, S., Muzi, P., Pavan, A., and Bologna, M. (1998) Plasminogen activator system modulates invasive capacity and proliferation in prostatic tumor cells. *Clin. Exp. Metastasis 16*, 513−528.
(61) Sprecher, C. A., Kisiel, W., Mathewes, S., and Foster, D. C. (1994) Molecular-cloning, expression, and partial characterization of a second human tissue-factor-pathway inhibitor. *Proc. Natl. Acad. Sci. U.S.A. 91*, 3353−3357.
(62) Miyagi, Y., Koshikawa, N., Yasumitsu, H., Miyagi, E., Hirahara, F., Aoki, I., Misugi, K., Umeda, M., and Miyazaki, K. (1994) cDNA cloning and mRNA expression of a serine proteinase-inhibitor secreted by cancer-cells: Identification as placental protein-5 and tissue factor pathway inhibitor-2. *J. Biochem. 116*, 939−942.
(63) Rao, C. N., Reddy, P., Liu, Y. Y., OToole, E., Reeder, D., Foster, D. C., Kisiel, W., and Woodley, D. T. (1996) Extracellular matrix-associated serine protease inhibitors (Mr 33,000, 31,000, and 27,000) are single-gene products with differential glycosylation: cDNA cloning of the 33-kDa inhibitor reveals its identity to tissue factor pathway inhibitor-2. *Arch. Biochem. Biophys. 335*, 82−92.
(64) Petersen, L. C., Sprecher, C. A., Foster, D. C., Blumberg, H., Hamamoto, T., and Kisiel, W. (1996) Inhibitory properties of a novel human Kunitz-type protease inhibitor homologous to tissue factor pathway inhibitor. *Biochemistry 35*, 266−272.
(65) Schechte., I., and Berger, A. (1967) On size of active site in proteases. I. Papain. *Biochem. Biophys. Res. Commun. 27*, 157−162.
(66) Bajaj, M. S., Ogueli, G. I., Kumar, Y., Vadivel, K., Lawson, G., Shanker, S., Schmidt, A. E., and Bajaj, S. P. (2011) Engineering kunitz domain 1 (KD1) of human tissue factor pathway inhibitor-2 to selectively inhibit fibrinolysis properties of KD1-L17R variant. *J. Biol. Chem. 286*, 4329−4340.
(67) Sambrook, J., and Russel, D. W. (2001) *Molecular Cloning: A Laboratory Manual*, 3rd ed., Cold Spring Harbor Laboratory Press, Cold Spring Harbor, NY.
(68) Chand, H. S., Schmidt, A. E., Bajaj, S. P., and Kisiel, W. (2004) Structure-function analysis of the reactive site in the first Kunitz-type domain of human tissue factor pathway inhibitor-2. *J. Biol. Chem. 279*, 17500−17507.
(69) Schmidt, A. E., Chand, H. S., Cascio, D., Kisiel, W., and Bajaj, S. P. (2005) Crystal structure of Kunitz domain 1 (KD1) of tissue factor pathway inhibitor-2 in complex with trypsin. Implications for KD1 specificity of inhibition. *J. Biol. Chem. 280*, 27832−27838.
(70) Stone, M. J., Ruf, W., Miles, D. J., Edgington, T. S., and Wright, P. E. (1995) Recombinant soluble human tissue factor secreted by Saccharomyces cerevisiae and refolded from Escherichia coli inclusion-bodies: Glycosylation of mutants, activity and physical characterization. *Biochem. J. 310*, 605−614.
(71) Laemmli, U. K. (1970) Cleavage of structural proteins during assembly of head of bacteriophage-t4. *Nature 227*, 680−685.
(72) Bieth, J. G. (1984) In vivo significance of kinetic constants of protein proteinase-inhibitors. *Biochem. Med. Metab. Biol. 32*, 387−397.
(73) Morrison, J. F., and Walsh, C. T. (1988) The behavior and significance of slow-binding enzyme-inhibitors. *Adv. Enzymol. Relat. Areas Mol. Biol. 61*, 201−301.
(74) Sperzel, M., and Huetter, J. (2007) Evaluation of aprotinin and tranexamic acid in different in vitro and in vivo models of fibrinolysis, coagulation and thrombus formation. *J. Thromb. Haemostasis 5*, 2113−2118.
(75) Henry, D. A., Carless, P. A., Moxey, A. J., O'Connell, D., Stokes, B. J., McClelland, B., Laupacis, A., and Fergusson, D. (2007) Anti-fibrinolytic use for minimising perioperative allogeneic blood transfusion. *Cochrane Database Syst. Rev. 16*, CD001886.
(76) Medynski, D., Tuan, M., Liu, W., Wu, S. L., and Lin, X. L. (2007) Refolding, purification, and activation of miniplasminogen and microplasminogen isolated from E-coli inclusion bodies. *Protein Expression Purif. 52*, 395−402.
(77) Hudig, D., and Bajaj, S. P. (1982) Tissue factor-like activity of the human monocytic tumor cell line U937. *Thromb. Res. 27*, 321−332.
(78) Felez, J., Miles, L. A., Plescia, J., and Plow, E. F. (1990) Regulation of plasminogen receptor expression on human monocytes and monocytoid cell lines. *J. Cell. Biol. 111*, 1673−1683.
(79) Halfman, C. J. (1981) Concentrations of binding protein and labeled analyte that are appropriate for measuring at any analyte concentration range in radioimmunoassays. *Methods Enzymol. 74*, 481−497.
(80) Cheng, Y., and Prusoff, W. H. (1973) Relationship between inhibition constant (K_I) and concentration of inhibitor which causes 50% inhibition (I_{50}) of an enzymatic reaction. *Biochem. Pharmacol. 22*, 3099−3108.
(81) Craig, D. A. (1993) The Cheng−Prusoff relationship: Something lost in the translation. *Trends Pharmacol. Sci. 14*, 89−91.
(82) Plow, E. F., Doeuvre, L., and Das, R. (2012) So many plasminogen receptors: Why? *J. Biomed. Biotechnol. 2012*, 141806-1−141806-6.
(83) Parry, M. A. A., Fernandez-Catalan, C., Bergner, A., Huber, R., Hopfner, K. P., Schlott, B., Guhrs, K. H., and Bode, W. (1998) The ternary microplasmin-staphylokinase-microplasmin complex is a proteinase-cofactor-substrate complex in action. *Nat. Struct. Biol. 5*, 917−923.
(84) Mathews, I. I., Vanderhoff-Hanaver, P., Castellino, F. J., and Tulinsky, A. (1996) Crystal structures of the recombinant kringle 1 domain of human plasminogen in complexes with the ligands epsilon-aminocaproic acid and trans-4-(aminomethyl)cyclohexane-1-carboxylic acid. *Biochemistry 35*, 2567−2576.
(85) Bajaj, M. S., Birktoft, J. J., Steer, S. A., and Bajaj, S. P. (2001) Structure and biology of tissue factor pathway inhibitor. *Thromb. Haemostasis 86*, 959−972.
(86) Eswar, N., Marti-Renom, M. A., Webb, B., Madhusudhan, M. S., Eramian, D., Shen, M., Pieper, U., and Sali, A. (2006) Comparative protein structure modeling with MODELLER, *Current Protocols in Bioinformatics*, pp 5.6.1−5.6.30, John Wiley & Sons, Inc., New York.
(87) Brooks, B. R., Bruccoleri, R. E., Olafson, B. D., States, D. J., Swaminathan, S., and Karplus, M. (1983) CHARMM: A program for macromolecular energy, minimization, and dynamics calculations. *J. Comput. Chem. 4*, 187−217.
(88) Bode, W., Turk, D., and Karshikov, A. (1992) The refined 1.9-Å X-ray crystal-structure of D-Phe-Pro-Arg chloromethylketone-inhibited human α-thrombin: Structure analysis, overall structure, electrostatic properties, detailed active-site geometry, and structure-function relationships. *Protein Sci. 1*, 426−471.
(89) Chang, J. Y. (1985) Thrombin specificity. Requirement for apolar amino acids adjacent to the thrombin cleavage site of polypeptide substrate. *Eur. J. Biochem. 151*, 217−224.

(90) Markus, G., Depasquale, J. L., and Wissler, F. C. (1978) Quantitative determination of binding of epsilon-aminocaproic acid to native plasminogen. *J. Biol. Chem. 253*, 727−732.
(91) Groh, J., Welte, M., Azad, S. C., and Kratzer, M. A. A. (1993) Monitoring of hemostasis during liver surgery. *Infusionstherapie 20*, 173−179.
(92) Schlag, M. G., Hopf, R., and Redl, H. (2000) Convulsive seizures following subdural application of fibrin sealant containing tranexamic acid in a rat model. *Neurosurgery 47*, 1463−1467.
(93) Lecker, I., Wang, D. S., Romaschin, A. D., Peterson, M., Mazer, C. D., and Orser, B. A. (2012) Tranexamic acid concentrations associated with human seizures inhibit glycine receptors. *J. Clin. Invest. 122*, 4654−4666.
(94) Makhija, N., Sarupria, A., Choudhary, S. K., Das, S., Lakshmy, R., and Kiran, U. (2013) Comparison of epsilon aminocaproic acid and tranexamic acid in thoracic aortic surgery: Clinical efficacy and safety. *J. Cardiothorac. Vasc. Anesth. 27*, 1201−1207.
(95) Manji, R. A., Grocott, H. P., Leake, J., Ariano, R. E., Manji, J. S., Menkis, A. H., and Jacobsohn, E. (2012) Seizures following cardiac surgery: The impact of tranexamic acid and other risk factors. *Can. J. Anaesth. 59*, 6−13.
(96) Kempaiah, P., Danielson, L. A., Barry, M., and Kisiel, W. (2009) Comparative effects of aprotinin and human recombinant R24K KD1 on temporal renal function in Long−Evans rats. *J. Pharmacol. Exp. Ther. 331*, 940−945.